ANALYSIS OF THE FIXED BED REACTOR FOR DME SYNTHESIS

Daesung Song[a], Sung Joon Ahn[a], Wonjun Cho[b], Dal Keun Park[a] and En Sup Yoon[a]

[a]School of Chemical Engineering, Seoul National University
San 56-1 Sillim-dong, Gwanak-gu, Seoul, Korea
[b]LNG Technology Research Center, KOGAS
Dongchun-dong, Yeonsu-gu, Incheon, Korea

ABSTRACT

Dimethyl Ether (DME, CH_3OCH_3) is the simplest ether and is considered as one of the leading candidates in the quest for a substitute for petroleum-based fuels. In this work, we analyzed the one-step synthesis of DME in a shell and tube type fixed bed reactor and carried out a simulation with a one-dimensional, steady state model of a heterogeneous catalyst bed, while taking into consideration the heat and mass transfer between the catalyst pellets and reactants gas and the effectiveness factor of the catalysts, together with the reactor cooling through the reactor tube wall. The reactor simulation was carried out under steady state condition and we compared the simulation results with the experimental data obtained from operations of a pilot-scale reactor and found good agreement between them.

Keywords: Reactor, Modelling, DME

1. INTRODUCTION

Dimethyl ether (DME), the simplest ether, is considered as a substitute fuel that could potentially replace petroleum-based fuels [1]. Its physical properties are similar to those of liquefied petroleum gas (LPG), so it can exploit the existing land-based and ocean-based LPG infrastructures with minor modifications. DME with its cetane number of 55 to 60 is also considered as a substitute for diesel fuel (cetane number 55)[2-5]. Compared with diesel fuel, the combustion of DME produced much less pollutants such as hydrocarbons, carbon monoxide, nitrogen oxides and particulates in CIDI engine tests [5, 6-9]. DME has been traditionally produced by the dehydration of methanol, which is produced from syngas, a product of natural gas reforming. This traditional process is thus called the two-step method of preparing DME. However, DME can also be prepared directly from syngas (single-step) [10-12]. The single-step method needs only one reactor for the synthesis of DME, instead of two for the two-step process. It can also alleviate the thermodynamic limitations associated with the synthesis of methanol, by converting the produced methanol into DME, thereby potentially enhancing the overall conversion of syngas into DME. In a fixed bed reactor, the main difficulty would be the prevention of the occurrence of hot spots, since the reactions involved in the synthesis of DME are highly exothermic. Catalysts can be irreversibly deactivated when they are exposed to certain temperatures. Therefore, it is necessary to understand and predict the behavior of the reactor under various conditions for the design and scale-up of the DME synthesis process. However, it is not feasible to gather all the data experimentally and, therefore, numerical simulations would be highly valuable in the development of such a process. In this study, we developed a mathematical model to simulate a pilot-plant scale shell and tube type DME reactor and analyzed the one-step synthesis of DME, and carried out the simulation of a pilot scale fixed bed reactor with a one-dimensional heterogeneous reactor model under steady state conditions, while considering the heat and mass transfer between the catalyst pellets and reactant gas and the effectiveness factor of the catalysts, together with the cooling of the reactor through the reactor wall. We used the hybrid catalyst which is, according to our definition, catalyst pellets prepared from a mixture of a fine powdered commercial methanol synthesis catalyst, $CuO/ZnO/Al_2O_3$, and a fine powdered methanol dehydration catalyst, γ-alumina. Thus, the active sites for the synthesis of methanol and those for its dehydration are inter-mixed within the catalyst pellets. Using the simulator developed in this study, we compared the experimental data from operations of a pilot-scale DME reactor with the simulation results, such as the temperature profile, CO conversion, DME yield and out stream composition.

2. REACTOR MODEL DEVELOPMENT

2.1 Reaction kinetics

Preparation of DME from syngas can be represented by three catalytic reactions as shown below. [13]

$$CO_2 + 3H_2 \longleftrightarrow CH_3OH + H_2O \qquad (1a)$$

$$CO + H_2O \longleftrightarrow CO_2 + H_2 \qquad (1b)$$

$$2CH_3OH \longleftrightarrow CH_3OCH_3 + H_2O \qquad (1c)$$

Reaction (1a) corresponds to the synthesis of methanol from carbon dioxide and hydrogen. Reaction (1b) is the water gas shift reaction. These two reactions are catalyzed by the methanol synthesis catalyst ($CuO/ZnO/Al_2O_3$). Reaction (1c) is the methanol dehydration reaction, i.e. the DME synthesis reaction catalyzed by an acidic catalyst (γ-alumina). Combinations of these three reactions can explain the other schemes of preparation of DME from syngas. We also use the reaction rate equations as follows [14, 15].

$$r_{CO_2 hydrogenation} =$$

$$\frac{k_1(p_{H_2}p_{co_2})[1-(1/K_{eqm1})(p_{CH_3OH}p_{H_2O})/(p_{CO_2}p_{H_2}^3)]}{(1+K_2(p_{H_2O}/p_{H_2})+\sqrt{K_3p_{H_2}}+K_4p_{H_2O})^3}$$

$$\Delta Hr = -49.47 kJ/mol \qquad (2a)$$

$$r_{RWGS} = \frac{k_5 p_{CO_2}[1-K_{eqm2}(p_{CO}p_{H_2O}/p_{CO_2}p_{H_2})]}{1+K_2(p_{H_2O}/p_{H_2})+\sqrt{K_3p_{H_2}}+K_4p_{H_2O}}$$

$$\Delta Hr = 41.17 kJ/mol \qquad (2b)$$

$$r_{MeOHdehydration} =$$

$$k_6K_{CH_3OH}^2[\frac{C_{CH_3OH}^2-(C_{H_2O}C_{DME}/K_{eqm3})}{(1+2\sqrt{K_{CH_3OH}C_{CH_3OH}}+K_{H_2O}C_{H_2O})^4}]$$

$$\Delta Hr = -21.003 kJ/mol \qquad (2c)$$

These three reactions are all exothermic. Therefore, the handling of the reaction heat is very important for the control of the reactions. The values of the kinetic parameters in the kinetic expressions are summarized in Table 2.1. The equilibrium constant of each reaction is taken from the literature [16, 17].

Table 2.1. kinetic parameters

	A(i)	B(i)	parameter
k_1	1.65	36696	4846.93
K_2	3610	0	3610
K_3	0.37	17197	15.61
K_4	7.14×10^{-11}	124119	38.34
k_5	1.09×10^{10}	-94765	12.07
K_{ch3oh}	0.00079	70500	3633.13
k_6	3.7×10^{10}	-105000	4.417
K_{H20}	0.084	41100	643.376

$parameter = A(i)\exp(B(i)/RT)$

$$Log_{10}K_{eqm1} = \frac{3066}{T} - 10.592 \qquad (3a)$$

$$Log_{10}\frac{1}{K_{eqm2}} = -\frac{2073}{T} + 2.029 \qquad (3b)$$

$$Log_{10}K_{eqm3} = \frac{10194}{T} - 13.91 \qquad (3c)$$

2.2 Heat and Mass Transfer on the surface of the catalyst

Due to the highly exothermic nature of the reactions, the temperature of the catalyst pellets can differ from that of the bulk stream of the reactants. Likewise, there could be a difference in the concentration of the reactants between the bulk and catalyst pellets surface. The heat and mass transport rate correlations on the surface of the catalyst are summarized as shown below.

$$N_{nu} = \frac{h_p d_p}{k_g} = 2 + 0.6 N_{\mathrm{Re}\,sph}^{0.5} N_{pr}^{1/3} \qquad (4)$$

$$N_{\mathrm{Re}\,sph} = \frac{d_p v \rho}{\mu}$$

$$N_{pr} = \frac{C_p \mu}{k_g}$$

$$\sum_i r_i \Delta H_r g_{cat} = h_p A_p (T_{p1} - T_f) \qquad (5)$$

2.3 Effectiveness factor

The intrinsic reaction rate can differ from the global reaction rate, because of pore diffusion in the catalyst pellets when their diameter is of the order of several millimeters. We assume that the temperature of each catalyst pellet is uniform and equal to the temperature on its surface and consider only the mass balance within it. For spherical catalyst pellets the concentration of the reactants and products can be obtained by solving the following partial different equations.[21].

$$\frac{d^2 C_{H_2}}{dr^2} + \frac{2}{r}\frac{dC_{H_2}}{dr} = \frac{3\rho_{p_1}}{D_{eff.H_2}} r_{CO_2} + \frac{\rho_{p_1}}{D_{eff.H_2}} r_{RWGS} \qquad (6a)$$

$$\frac{d^2 C_{CO}}{dr^2} + \frac{2}{r}\frac{dC_{CO}}{dr} = -\frac{\rho_{p_1}}{D_{eff.CO}} r_{RWGS} \qquad (6b)$$

$$\frac{d^2 C_{CO_2}}{dr^2} + \frac{2}{r}\frac{dC_{CO_2}}{dr} = \frac{\rho_{p_1}}{D_{eff.CO_2}} r_{CO_2} + \frac{\rho_{p_1}}{D_{eff.CO_2}} r_{RWGS} \qquad (6c)$$

$$\frac{d^2 C_{H_2O}}{dr^2} + \frac{2}{r}\frac{dC_{H_2O}}{dr} =$$

$$-\frac{\rho_{p_1}}{D_{eff.H_2O}} r_{CO_2} - \frac{\rho_{p_1}}{D_{eff.H_2O}} r_{RWGS} - \frac{\rho_{p_2}}{2D_{eff.H_2O}} r_{MeOH} \qquad (6d)$$

$$\frac{d^2 C_{DME}}{dr^2} + \frac{2}{r}\frac{dC_{DME}}{dr} = -\frac{\rho_{p_2}}{2D_{eff.DME}} r_{MeOH} \qquad (6e)$$

$$\frac{d^2 C_{MeOH}}{dr^2} + \frac{2}{r}\frac{dC_{MeOH}}{dr} = -\frac{\rho_{p_1}}{D_{eff.MeOH}} r_{CO_2} + \frac{\rho_{p_2}}{D_{eff.MeOH}} r_{MeOH} \qquad (6f)$$

Boundary conditions

$$r = R, C = C_o$$

$$r = 0, \frac{dC}{dr} = 0$$

The effective diffusivity of the gases through the porous catalyst pellets was estimated from the molecular diffusivity, porosity and tortuosity of the pores using equation (7). The solutions of these equations provide the concentration profiles of the gas species in the catalyst pellets together with the global reaction rates.

$$D_{eff.i} = D_i \frac{\varepsilon}{\tau} \qquad (7)$$

ε = *void fraction (porosity)*

τ = *tortuosity*

2.4 Heat transfer between tubes and shell

The heat generated from the chemical reactions in the catalyst is transferred to the gases flowing through the reactor tubes, and then to the cooling medium on the shell side of the reactor. Equation (8) holds for the whole reactor, as well as for any given section of it. It calculates the temperature rise of the reactants by subtracting the heat transferred to the coolant from the heat generated by the chemical reactions.

$$(\sum_i r_i \Delta H_r g_{cat} - U A_t (T_f - T_o)) = C_{p,fluid} m_f \Delta T_f \qquad (8)$$

In order to estimate the heat transfer coefficient (9a), U, we need to know both the shell side and tube side heat transfer coefficients. The common method of calculating the heat transfer coefficient can be employed for the

estimation of the shell side heat transfer coefficient (9b), as heat transferring liquid or boiling water is used as the cooling medium in the shell [22].

$$U_o = \frac{1}{\frac{1}{h_i}(\frac{D_o}{D_i}) + \frac{x_w}{k_m}(\frac{D_o}{D_L}) + \frac{1}{h_o} + \frac{D_o}{D_i}\frac{1}{h_{di}} + \frac{1}{h_{do}}} \quad (9a)$$

$$h_o = \frac{0.023 C_p v \rho}{N_{pr}^{2/3} N_{re}^{0.2}} \quad (9b)$$

However, the presence of the catalyst pellets makes the estimation of the heat transfer coefficient on the tube side much more complicated. Although several correlations are available in the literature, their reliability should be experimentally verified. As we do not have experimental values for the tube side heat transfer coefficient, we selected the correlation (10) for the estimation of the tube side heat transfer coefficient [18].

$$h = (\frac{1}{\frac{1}{h_r + 2k_{ew}^0 / d_p + a_w C_{pg} \rho_g v} + \frac{1}{h_{packet}}}) \quad (10)$$

$$h_{packet} = 1.13(\frac{k_e^0 \rho_p (1-\varepsilon_{mf}) C_{ps}}{\tau_t})^{0.5}$$

$$k_{ew}^0 = \varepsilon_w k_g + (1-\varepsilon_w) k_s (\frac{1}{\phi_w (k_s / k_g) + 1/3})$$

$$k_e^0 = \varepsilon_{mf} k_g + (1-\varepsilon_{mf}) k_s (\frac{1}{\phi_b (k_s / k_g) + 2/3})$$

$$a_w = 0.05, h_r(radiation) = 0$$

2.4 Simulation of the reactor

Equation (11) is used to calculate the mass flowrate profile in the tube of the reactor [23].

$$\frac{dF_i}{dz} = \rho_b \frac{\pi D_j^2}{4} \sum_{j=1}^{n_r} \gamma_{i,j} r_j \quad i = 1,2,..,n_c \quad (11)$$

In order to solve the above ODE, the axial length of the reactor tube is divided into 1000 sections. First, the reaction rates are calculated with the use of the correlations listed in section 2.1. For this calculation, the heat and mass transfer on the surface of the catalyst described in section 2.2 and the effectiveness factor described in section 2.3 are incorporated in order to reflect their effects on the reaction rates. Then, the correlations of section 2.4 are used for the calculation of the reactor temperature in each section. Iterative procedures for determining the temperature and reaction rates in each section are necessary, as the temperature and reaction rates are inter-dependent. After determining the temperature in the section of the tube, the mass balance in each section is calculated using Equation (11) and then the simulation is allowed to proceed to the next step.
We used the following correlations to evaluate the reactor performance, such as the CO conversion and DME Yield:

$$COconversion = \frac{COin - COout}{COin} \times 100 \quad (12a)$$

$$DMEyield = \frac{DMEout \times 2}{COin - COout} \times 100 \quad (12b)$$

3. RESULTS AND DISCUSSION

Using the simulator we developed, the behavior of a pilot-scale DME reactor was studied. The base condition of the reactor for the simulation is as follows: feed composition (yH2 = 0.653, yCO = 0.326, yCO2 = 0.003, yCH4 = 0.0025, yH2O = 0.0155, yCH3OCH3 = 0, yCH3OCH3 = 0), GHSV 2000 hr^{-1}, feed temperature 220 ℃, reactor pressure 50 bar, H_2 : CO ratio 2:1, inlet temperature of cooling water 210 ℃. The hybrid catalyst consists of the methanol synthesis and methanol dehydration components, whose ratio is 8:2. We compared the

experimental data obtained from the pilot scale fixed bed reactor using the hybrid catalyst with the simulation results.

3.1 Comparison of experimental data and simulations result

The properties of the catalyst and the in formation concerning the pilot-plant scale reactor are shown in Table 3.1. These data were used for the simulation of the reactor.

Table3.1. Property of catalyst and the pilot-plant scale reactor

Catalyst	Density (kg/m_3)	1783.5
	Porosity (%)	45.53
	Pore tortuosity	1.69
	Mass (kg)	7.85
	Pellet diameter (m)	0.006
Reactor	Tube diameter (m)	0.03
	Length (m)	1.6
	Tube number	7

Fig. 3.1 shows the simulated temperature profile and the reactor temperature at 5 points (0.16 m, 0.608 m, 1.08 m). Although the simulated temperature profile has an error range of within ±8.8°C, this simulator can predict the temperature profile of the reactor well, thus helping to control the temperature of the reactor and preventing the irreversible deactivation of the catalysts.

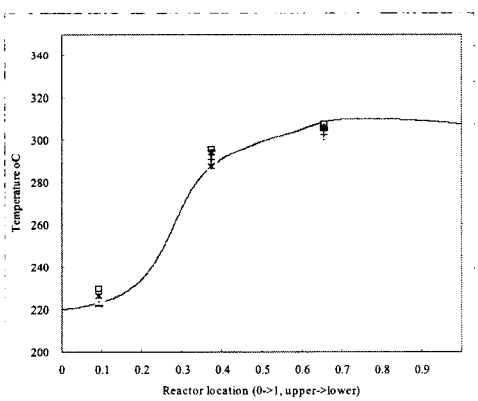

Fig. 3.1. Simulated temperature profile and the experimental data of the reactor filled with only hybrid catalyst

Table 3.2 shows the simulation result with corresponding pilot plant reactor data. As can be seen there is a good agreement between the simulations result and pilot plant reactor data.

Table3.2. Comparison of the simulation result and pilot plant reactor data

Property	Simulation result	Pilot plant result 1	Pilot plant result 2	Pilot plant result 3	Pilot plant result 4	Pilot plant result 5
CO conversion	39.85	39.4	38.93	37.92	37.39	36.27
DME yield	50.58	50.02	49.41	48.01	47.20	45.39
Exit temp.(℃)	307	312	309	308	308	309
Mole %						
yH_2	54.96	54.74	56	54	57	53
yCO	29.6	29.8	29.9	30.3	28.4	32.61
yCO_2	6.79	6.68	5.42	7.31	6.17	5.88
yCH_4	0.31	0.31	0.30	0.24	0.31	0.31
yH_2O	0.43	0.41	0.39	0.36	0.34	0.31
yCH_3OCH_3	4.97	4.78	4.71	4.44	4.29	3.98
yCH_3OH	2.94	3.02	3.12	3.33	3.45	3.71

Byproduct	0.26	0.16	0.02	0.04	0.2

4. CONCLUSION

In this work, we developed a simulator of a shell and tube type pilot-scale fixed bed reactor for the single-step synthesis of DME from syngas by applying the one-dimensional heterogeneous model under the steady state. We examined the behavior of the reactor in the hybrid catalyst. We found that complex reactions coupled with pore diffusion within the catalyst pellets can result in unusual values of the effectiveness factor. Therefore, the reactor showed higher performance. However, more careful cooling is needed due to reaction heat. We applied this model to a pilot-scale reactor and found that there was good agreement between the simulation result and experimental data. We were also able to predict the behavior of the reactor using this simulator. In this way, we were able to predict the temperature profile of the reactor and prevent the irreversible deactivation of the catalyst, thus allowing stable and optimized operation conditions to be obtained and the scale up of the DME synthesis reactor to be achieved.

ACKNOWLEDGEMENTS

The support provided for this study by KOGAS (Korea Gas Corporation) and BK21 (Brain Korea21) is gratefully acknowledged.

REFERENCES

[1] Troy A. Semelsberger, Rodney L. Borup, Howard L. Greene., "Dimethyl ether (DME) as an alternative fuel" *J Power Sources* **156,** 497-511(2006).

[2] Alam M, Fujita O, Ito K., "Performance of NOx reduction catalysts with simulated dimethyl ether diesel engine exhaust gas" *Proc. Inst. Mech. Eng. Part A: J Power Energy* **218**, 89-96(2004).

[3] Sorenson SC., "Dimethyl ether in diesel engines: Progress and perspectives." *J Eng Gas Turbines Power-Trans ASME* **123**, 652-658(2001).

[4] Rouhi AM. AMOCO, "HALDOR-TOPSOE Develop Dimethyl Ether As Alternative Diesel Fuel" *Chem Eng News* **73**, 37-39(1995).

[5] Fleisch TH, Basu A, Gradassi MJ, Masin JG., "Dimethyl ether: A fuel for the 21st century" *Natural Gas Conversion IV Studies in Surface Science and Catalysis* **107**, 117-125(1997).

[6] E.W. Kaiser, T.J. Wailington, M.D. Hurley, J. Platz, H.J. Curran, W.J. PITZ, C.K. Westerbrook., "Experimental and modelling study of premixed atmospheric-pressure dimethyl ether-air flames" *J Phys Chem A* **104**, 8194-8206(2000).

[7] Song J, Huang Z, Qiao XQ, Wang WL. "Performance of a controllable premixed combustion engine fuelled with dimethyl ether" *Energy Convers Manage* **45**, 2223-2232(2004).

[8] Wang HW, Zhou LB., "Performance of a direct injection diesel engine fuelled with a dimethyl ether/diesel blend" *Proc. Inst Mech EngPart D: J Automobile Eng* 217, 819-824(2003).

[9] Zannis TC, Hountalas DT., "DI diesel engine performance and emissions from the oxygen enrichment of fuels with various aromatic content" *Energy Fuels* **18**, 659-666(2004).

[10] Peng XD, Wang AW, Toseland BA, Tijm PJA., "Single-Step Syngas-to Dimethyl Ether Processes for Optimal Productivity Minimal Emissions, and Natural Gas-Derived Syngas" *Ind Eng Chem Res* 38, 4381-4288(1999).

[11] Kunpeng Sun, Weiwei Lu, Fengyan Qiu, Shuwen Liu, Xianlun Xu., "Direct synthesis of DME over bifunctional catalyst: surface properties and catalytic performance" *Applied Catalysis A: General* **252**, 243-249(2003).

[12] Kohji Omata, Yuhsuke Watanabe, Tetsuo Umegaki, Gunji Ishiguro, Muneyoshi Yamada., "Low-pressure DME synthesis with Cu-based hybrid catalysts using temperature-gradient reactor" *Fuel* **81**, 1605-1609(2002).

[13] Ng KL, Chadwick D, Toseland BA., "Kinetics and modelling of dimethyl ether synthesis from synthesis gas" *Chem Eng Sci* **54**, 3587-3592(1999).

[14] Vanden Busshe KM, Froment GF., "A steady-state kinetic model for methanol synthesis and the water gas shift reaction on a commercial $Cu/ZnO/Al_2O_3$ catalyst" *J Catalyst* **161**, 1-10(1996).

[15] Gorazd Bercic, Janez Levec., "Intrinsic and Global reaction rate of methanol dehydration over γ-Al_2O_3 pellets" *Ind Eng Chem Res* **31**, 1035-1040(1992).

[16] Martyn V., Twigg. Catalyst Handbook, 2nd ed, Wolfe, London (1986).

[17] Daniel R. Stull, Edgar F. westrum. Jr, Gerard C. Sinke., The Chemical Thermodynamics of Organic Compounds, John Wiley , New York(1969).

[18] Daizo Kunii, Octave Levenspiel., Fluidization Engineering, 2nd ed, Butterworth-Heinemann , Boston(1990).

[19] James R. Welty, Charles E. Wicks, Robert E. Wilson., Fundamentals of momentum, heat and mass transfer, 3rd ed, Wiley , New York(1976).

[20] Cengel., Heat transfer a practical approach, 2nd ed, McGrawHill , Boston(1998).

[21] Charles N. Satterfield., Mass Transfer in Heterogeneous Catalysis, M.I.T. Press , Cambridge Mass(1970).

[22] Warren L.McCabe, Julian C.Smith, Peter Harriott., Unit Operations of Chemical Engineering, 5th ed, McGrawHill , New York(1995).

[23] Riggs, J.M., An introduction to numerical methods for chemical engineers, Texas Tech University Press , Lubbock(1994).